ESC-TR-97-060

Technical Report
1038

The Westford Water Vapor Experiment: Use of GPS to Determine Total Precipitable Water Vapor

A.J. Coster
A.E. Niell
H.K. Burke
M.G. Czerwinski

17 December 1997

Lincoln Laboratory
MASSACHUSETTS INSTITUTE OF TECHNOLOGY
LEXINGTON, MASSACHUSETTS

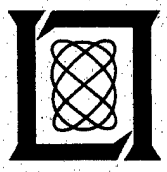

This research effort was supported under the auspices of the Lincoln Laboratory Advanced Concepts Program. The Advanced Concepts Program is supported principally by the Department of the Air Force under Contract F19628-95-C-0002.

This report is based on studies performed at Lincoln laboratory, a center for research operated by Massachusetts Institute of Technology. This work was supported under the auspices of the Lincoln Laboratory Advanced Concepts Program. The Advanced Concepts Program is supported principally by the Department of the Air Force under Contract F19628-95-C-0002.

The ESC Public Affairs Office has reviewed this report, and it is releasable to the National Technical Information Service, where it will be available to the general public, including foreign nationals.

This technical report has been reviewed and is approved for publication.

FOR THE COMMANDER

Gary Tattungian
Administrative Contracting Officer
Contracted Support Management

MASSACHUSETTS INSTITUTE OF TECHNOLOGY
LINCOLN LABORATORY

THE WESTFORD WATER VAPOR EXPERIMENT: USE OF GPS TO DETERMINE TOTAL PRECIPITABLE WATER VAPOR

A.J. COSTER
Group 91

A.E. NIELL
MIT Haystack Observatory

H.K. BURKE
Group 97

M.G. CZERWINSKI
Group 93

TECHNICAL REPORT 1038

17 DECEMBER 1997

LEXINGTON MASSACHUSETTS

EXECUTIVE SUMMARY

The Westford Water Vapor Experiment (WWAVE) was designed to measure the temporal and spatial variability of the total precipitable water vapor (PWV) over an area defined by an approximate 25 km radius centered on the Haystack Observatory in Westford, MA. PWV is defined as the height of liquid water that would result from condensing all the water vapor in a column from the Earth's surface to the top of the atmosphere. Such information can be used in climate and weather research. Water vapor is one of the most important greenhouse gases. Long-term changes in the amount of water vapor in the atmosphere need to be monitored to help detect and predict changes in the earth's climate.

The PWV measurement can also be used to improve weather forecasting. Atmospheric water vapor is a critical component in the formation of clouds, precipitation, and severe weather. Currently, the National Weather Service (NWS) obtains information on the water vapor distribution from both satellite information and from twice daily radiosonde launches at approximately 70 sites around the Continental U.S. The recovery of the PWV by satellites is complicated over land (not oceans) because of the variable surface temperature. The recovery of the PWV by radiosondes is fairly straightforward, however, the radiosonde network is expensive to operate, and there are currently proposals to reduce the number of operational sites in the U.S. In addition, balloons carrying the sonde packages take about an hour to reach the tropopause and can drift over an area of 100 square km. As a result, radiosonde data do not represent actual vertical water vapor profiles. Finally, with the current network, the horizontal spatial density is too low (70 sites) and time between launches too long (12 hours) to observe rapid changes of the water vapor with time and position.

The Global Positioning System (GPS) has the potential of providing a continuous measurement of the average total precipitable water vapor around a site on a near real-time basis (half-hour). Once installed, a GPS receiver can run automatically, and additional costs are associated primarily with data processing. The type of information provided by GPS can close the 12-hour gap and allow for better spatial distribution in the network. It has been shown [1] that when a PWV time series was introduced into the NCAR/Penn State mesoscale model, the accuracy of short-range precipitation forecasts was significantly improved. The assimilation of precipitable water vapor improved the rms errors in the initial moisture analysis—a key component of the forecast model—by 20%. The additional inclusion of surface humidity data further reduced this rms error by as much as 40%.

The main experiment associated with WWAVE was conducted from 15 August to 30 August 1995, and a variety of different techniques were used to measure the water vapor, including: radiosondes launched two to three times daily from one location; a water vapor radiometer (WVR); and 11 GPS receivers separated by 0.5 to 40 km. Three of the receivers were located within 1 km of both the WVR and radiosonde launch sites. Surface meteorological monitoring units were collocated at eight of the GPS sites. In addition, estimates of the precipitable water vapor were obtained with the Westford antenna as

part of a six-station Very Long Baseline Interferometry (VLBI) network that also included antennas in Alaska, Hawaii, Germany, Sweden, and Norway.

The primary goal of WWAVE was to evaluate the accuracy of the GPS PWV measurement and to analyze the issues involved in determining this accuracy. However, an absolute assessment of the GPS PWV measurement is not possible because a measurement technique capable of determining the absolute "true" value of PWV does not exist. This was evidenced in the comparison of the various PWV measurement techniques used during WWAVE. All methods have calibration issues. For example, discrepancies on the order of 10-30 mm of zenith wet delay (1-5 mm of PWV) were seen when PWV measurements obtained by radiosondes launched at Haystack were compared to those obtained from the nearest NWS radiosonde sites (Grey, Maine; Chatham, Massachusetts; and Albany, New York). Possible explanations include differences in geographical locations, humidity sensors used by the different sonde manufacturers (Viz vs Vaisala), and/or processing algorithms. In addition, a comparison of the collocated Haystack radiosonde and WVR estimates of PWV also indicated differences on the order of 10 mm wet zenith delay (1-2 mm of PWV). These differences can possibly be attributed to the retrieval coefficients used to solve for the WVR estimate of PWV, which are based on a fit to three months of NWS sonde data (the Haystack sonde data set was too limited to be used for determining retrieval coefficients). Finally, systematic differences in the GPS determination of PWV were observed that depend on the elevation cutoff used in the GPS analysis. These differences were not specific to the type of GPS antenna or receiver and were not seen at all sites. The discrepancies are consistent with the effects of near-field scattering seen in geodetic GPS measurements and indicate that GPS antenna mounts should be considered in designing water vapor retrieval systems based on GPS. This last finding is directly applicable to the real-time determination of PWV using GPS data and is discussed in the last section of this report, along with other implications concerning the types of GPS receivers and antennas used for real-time determination of PWV.

In the final analysis, GPS estimates of zenith wet delay agree with measurements by WVR and radiosondes to within 6-12 mm, corresponding to 1-2 mm of PWV. The GPS data presented here were all taken with either Allen Osborne Associates (AOA) Turbo Rogue GPS receivers with Dorne-Margolin choke ring antennas or with Ashtech Z12 GPS receivers equipped with either a choke ring antenna or with an older Ashtech surveying antenna. An elevation cutoff of 5 degrees was used for the data analysis involving instrument accuracy comparison. The comparisons of PWV accuracy determined in WWAVE are consistent with the results of GPS/STORM [2], even though they used an elevation cutoff of 15 degrees and different receivers and antennas. Furthermore, DoD's anti-spoofing (AS) had not been turned on during GPS/STORM, while it had been during WWAVE. The precision of the GPS measurement of ZWD is better than 6 mm (1 mm of PWV) as shown by the agreement of three closely spaced GPS systems.

ACKNOWLEDGMENTS

Numerous people helped us during the course of this experiment. We would especially like to recognize Virgilio Mendes and Pieter Toor of the University of New Brunswick, Canada; and Craig Richard and Karl Buchmann of MIT Lincoln Laboratory who helped us set up and collect data from the various sites throughout this experiment. In addition, Carolyn Upham of MIT Lincoln Laboratory played a substantial role in the data analysis. Fred Solheim of the Radiometrics Corporation provided the WVR and the Paroscientific Barometers. Richard Langley of the University of New Brunswick, Canada, lent us not only his graduate students, but also two GPS receivers. Frank Colby of the University of Massachusetts at Lowell arranged for his Vaisala surface meteorology measurements and helped us gain access to a roof. Tom Caudill and Artie Jackson of Phillips Laboratory provided us with Vaisala surface meteorology measurements and radiosonde data. Jim Ryan of the Goddard Space Flight Center supplied the VLBI zenith wet delay estimates. We would also like to recognize the loan of GPS receivers from Miranda Chin and Gerry Mader of NOAA; Jan Johansson and Jim Davis of Harvard Smithsonsian Center for Astrophysics; Tom Herring, Bob King, and Rob Reilinger of MIT; and Mike Pratt and Pratap Misra of MIT Lincoln Laboratory. Sandy Johnson, Jim Hunt, Andy Cott, Larry Swezey, the Groton Fire Tower, the Nashoba Vocational Technical High School, and the University of Massachusetts at Lowell all allowed us to use their roofs or towers. Finally, we would like to express our gratitude to Bernadette Johnson and the ACC Committee of MIT Lincoln Laboratory for their support.

TABLE OF CONTENTS

LIST OF ILLUSTRATIONS

LIST OF ILLUSTRATIONS (Continued)

LIST OF TABLES

1. INTRODUCTION

The Westford Water Vapor Experiment (WWAVE) was designed to investigate the use of the Global Positioning System (GPS) to determine total precipitable water vapor (PWV). PWV is defined as the height of liquid water that would result from condensing all the water vapor in a column from the Earth's surface to the top of the atmosphere. Such information can be used in climate and weather research. Water vapor is one of the most important greenhouse gases. Long-term changes in the amount of water vapor in the atmosphere need to be monitored to help detect and predict changes in the earth's climate.

The PWV measurement can also be used to improve weather forecasting [1]. Atmospheric water vapor is a critical component in the formation of clouds, precipitation, and severe weather. Currently, the National Weather Service (NWS) obtains information on the water vapor distribution from satellite information and from twice daily radiosonde launches at 70 sites around the Continental U.S. The recovery of the PWV by satellites is complicated over land (not oceans) because of the variable surface temperature. The radiosonde network is expensive to operate, and there are currently proposals to reduce the number of operational sites in the U.S. The balloons carrying the sonde packages take about an hour to reach the tropopause and can drift over an area of 100 square km. As a result, radiosonde data are not available on time scales of less than an hour, and the measurements do not represent actual vertical water vapor profiles. In addition, the horizontal spatial density is too low and time between launches too long to observe rapid changes of the water vapor with time and position. GPS can provide a continuous measurement on a near real-time basis (half-hour) of the average total precipitable water vapor around a site. Once installed, a GPS receiver can run automatically, and additional costs are associated primarily with data processing. The type of information provided by GPS can close the 12-hour gap and allow for better spatial distribution in the network.

GPS data are used to estimate the zenith tropospheric delay from measurements of the delay to each GPS satellite in view from a ground station. Typically, six to nine GPS satellites are in view at any given time over the Continental U.S. A global network of GPS receivers is required to determine both the GPS orbits and the additional biases introduced by the satellite and receiver clocks. The analysis of GPS data produces an estimate of zenith wet delay, ZWD. The zenith wet delay is the part of the range delay that can be attributed to the water vapor in the troposphere. PWV is related to ZWD by a factor that is approximately 0.15 [3]. This factor varies by 20% and is a function of the weighted mean temperature of the atmosphere [4]. It can be determined to about 2% when it is computed as a function of surface temperature, and to about 1% if data from numerical weather models are used. The zenith wet delay, ZWD, in the Westford, Massachusetts, area ranges from near 0 to approximately 40 cm, corresponding to a PWV of 0 to 6 cm. The data presented in this report are given in terms of zenith wet delay.

The primary goal of WWAVE was to estimate the total precipitable water vapor from GPS data and to evaluate the accuracy of these estimates. WWAVE consisted of a one month campaign using a network of ground-based GPS receivers to recover the total precipitable water vapor at individual stations. The 11 GPS sites are within 25 km of Haystack Observatory, which is located in Westford, Massachusetts. In order to evaluate the accuracy of the GPS measurement of PWV, GPS estimates were compared to those from water vapor radiometers (WVRs), very long baseline interferometry (VLBI), and radiosondes. In addition, three Allen Osborne Associates Turbo Rogue GPS receivers with Dorne-Margolin choke ring antennas were sited approximately 1 km apart at the central Westford location. The close positioning of these receivers, referred to in this report as WFRD, WES2, and MHR0, enabled the measurement of variations in the GPS PWV estimate that can be attributed to multipath or instrumental differences rather than the spatial or temporal differences in PWV.

A secondary goal of WWAVE was to examine issues involved in the real-time determination of PWV. A brief summary of the work being done by other groups will be presented. This report focuses on the effect of different types of GPS receivers, and GPS antennas and antenna mounts, on the retrieval process of PWV. To this end, different types of receivers and antennas were compared. An analysis of the effect of different elevation cutoffs of GPS data used in solving for the PWV is presented. In addition, a comparison made of the ionospheric delay term using data from the two different types of receivers is shown. While determination of the ionospheric delay is not directly related to the PWV measurement in GPS, it is a delay term that needs to be correctly accounted for. With the advent of anti-spoofing, the real-time determination of this quantity needs to be considered in some detail as it will impact the determination of PWV.

2. BACKGROUND

Since 1992, a combined group of scientists from UNAVCO, North Carolina State University (now at the University of Hawaii), and MIT have been investigating the use of GPS for the determination of total precipitable water vapor ([5],[2],[3],[6]). Earlier work [7] had indicated that GPS data could be used to recover the tropospheric path delay. Initial results from these experiments have been encouraging, although it is clear that issues remain in the area of data processing, real-time development, and accuracy. Several other groups have begun to look at these problems, including [8] who used a network of receivers located in the United Kingdom, Germany, Spain, Sweden, Finland, and the Netherlands.

In the GPS/STORM experiment [6] data were collected from six GPS receivers for a one month period in 1993 at sites in Colorado, Oklahoma, and Kansas. Four of these sites were also equipped with water vapor radiometers (WVR's). All of the GPS receivers used in GPS/STORM were Trimble^{TM} 4000 SST eight channel dual frequency phase and C/A code receivers. Most of their antennas were mounted 3 m high atop stable fence posts. One was mounted atop a trailer. A 15-degree elevation cutoff was used throughout the analysis of the GPS/STORM data. Because of this, the specific tropospheric mapping function used was not significant. Data were analyzed with the UNAVCO version of the GPS Bernaese V.3.4 software using GPS satellite orbits generated by the Center for Orbit Determination in Europe (CODE) in Berne, Switzerland. The analysis of these data indicated that water vapor can be monitored with an accuracy of 1-2 mm of PWV (6-12 mm of zenith wet delay) over a 900 km six receiver network. In their conclusion, they suggested that better GPS antennas could be installed at the sites to reduce multipath. In addition, a feasibility study was suggested to consider the operation of near real-time GPS meteorological monitoring networks. Finally, note that DoD anti-spoofing (AS) was not on during the GPS/STORM experiment. AS was on during WWAVE.

WWAVE was designed to use a geographically smaller array than the above groups. The GPS/STORM experiment had receivers scattered over several states, while WWAVE focused on a network of receivers within 25 km of the central Westford location. The majority of antennas used during WWAVE were Dorne-Margolin choke ring antennas. These antennas were designed to minimize the multipath problem, and their use allowed the inclusion of GPS data down to 5 degrees in elevation. In addition, the GPS processing software, GIPSY/OASIS [9], was updated with the Niell tropospheric mapping functions [10] described later in this report. The focus of the work presented here is on the accuracy of the GPS measurements of PWV. The issues examined concern the consistency of the GPS determined values of the zenith wet delay (ZWD) as compared to ZWD's derived from radiosondes and a WVR. In addition, the consistency of the GPS determined values of zenith wet delay among GPS receivers/antennas of the same type was studied by analyzing the data from three receivers located within 1 km of each other. WWAVE used improved P-code GPS receivers, specific antennas to reduce site multipath, and improved tropospheric mapping functions for estimation of the zenith wet delay.

3. THE GPS MEASUREMENT

GPS was designed as a navigation system. Each satellite carries an atomic clock and knows its own position in earth-centered earth-fixed coordinates. A simple description of how this system works is given here. The GPS satellite broadcasts a signal at two frequencies (L1 = 1575.42 MHz and L2 = 1227.6 MHz). A single receiver on the ground receives a coded signal from the GPS satellite from which it can obtain the time the GPS signal left the satellite plus the orbital position of the satellite at that time. For one satellite, assuming that the GPS signal traveled at the speed of light, the knowledge of the difference in time between when the GPS signal was sent from the satellite and when it was received on the ground, allows for the calculation of the receiver's location somewhere on the surface of a hypothetical sphere. To have the receiver's position pinpointed in three-dimensional space, at least three GPS satellites must be in view. A fourth satellite is needed to compute an offset to the receiver's clock. With the fully implemented GPS system of 24 satellites, there are always at least six satellites in view over the Continental U.S., and there can be as many as eleven, depending on user location and orbit inclination.

Obviously, this simple description neglects a number of additional factors that must be accounted for if precise positioning is required. First, the GPS signal does not travel at the speed of light, but rather at a slower speed corresponding to the group velocity of the wave. The group velocity is less than the speed of light in both the ionosphere and the troposphere. In the ionosphere, the index of refraction depends both on the frequency of the wave and on the total electron content. In the troposphere, the index of refraction depends on the pressure, temperature, and humidity. Because the ionospheric group delay is dispersive (dependent on frequency), use of a dual frequency GPS receiver is required for direct calculation of the ionospheric term. In addition to the atmospheric delays, other factors must be taken into account, including signal multipath (the type of antenna used plays a factor in multipath reduction), the receiver location, the satellite's true orbit (since the broadcast orbit is not very accurate), satellite clock offsets, and receiver clock offsets. To determine very precise GPS orbits, the effects of the gravitational potential, special relativistic shifts, and Doppler shifts must all be accounted for.

In this report, the GPS estimates of the zenith wet delay were computed using JPL's GIPSY/OASIS software [9], and the JPL determined precise orbits and corresponding satellite clocks were used. These orbits are predicted to be accurate to better than 20 centimeters [11]. Recent improvements to the software and analysis have led to orbits accurate at the 10-15 centimeter level [12].

3.1 TROPOSPHERIC RANGE DELAY

The excess path length due to travel in the troposphere, Δr_{trop}, at zenith, is defined to be:

$$\Delta r_{trop}(90^\circ) = 10^{-6}\int_{r_s}^{r_a} N(r)\,dr \tag{1}$$

where the refractivity, N, is related to the index of refraction, n, by $N = 10^6(n-1)$, r_s is the geodetic radius of the earth's surface, and r_a is the geodetic radius of the top of the neutral atmosphere [13]. By looking only at the zenith delay, the geometric delay term, Δr_{geo}, that accounts for the difference between the refracted and rectilinear ray paths can be neglected. Normally this term would need to be included in eqn. 1.

The refractivity of a parcel of air is given by the empirical formula [14]:

$$N = k_1\left(\frac{p_d}{T}\right)Z_d^{-1} + \left[k_2\left(\frac{p_v}{T}\right) + k_3\left(\frac{p_v}{T^2}\right)\right]Z_w^{-1}, \tag{2}$$

where T is the temperature in Kelvin, p_d is the partial pressure of the dry air, p_v is the partial pressure of water vapor in millibars, k_1 ,k_2 ,k_3 are empirically determined constants, Z_d is the compressibility factor for dry air, and Z_w is the compressibility factor for wet air. The first and second terms of this equation arise from electronic transitions of the induced dipole type for dry air molecules and water vapor, respectively. The third term arises from the permanent dipole rotational transitions of water vapor. The dry component of refractivity can be rewritten in terms of the total pressure as [4]:

$$N = k_1 R_d \rho + \left[k_2' \left(\frac{p_v}{T}\right) + k_3\left(\frac{p_v}{T^2}\right)\right] Z_w^{-1} \tag{3}$$

$$\text{where } k_2' = \left(k_2 - k_1\frac{M_w}{M_d}\right),$$

where M_w/M_d is ratio of the molar masses of water vapor and dry air, ρ is the total moist air density, and R_d is the specific gas constant for dry air. The above definition of the refractivity can be used to define a "hydrostatic" and a "wet" component of the tropospheric path delay at zenith, $\Delta r_{trop,hydro.}(90^\circ)$ and $\Delta r_{trop,wet}(90^\circ)$. A mapping function, $m(el)$, can then be used to compute the correction needed to convert the zenith delay term to one associated with the line of sight,

$$\Delta r_{trop}(el) = \Delta r_{trop}(90^\circ) m(el)\,. \tag{4}$$

However, the use of separate mapping functions for the "hydrostatic" and "wet" component of the excess path length is physically more correct and produces better estimates:

$$\Delta r_{trop}(el) = \Delta r_{trop,hydro.}(90^\circ) m_{hydro}(el) + \Delta r_{trop,wet}(90^\circ) m_{wet}(el)\,. \tag{5}$$

A global hydrostatic mapping function, $m_{hydro}(el)$ has been developed in [10] which has as inputs only the height above sea level, the latitude of the station, and the day of year. A wet mapping function, $m_{wet}(el)$, which is a function only of latitude, has also been generated in [10]. The separation of the wet from the hydrostatic term of tropospheric delay requires accurate surface barometric pressure readings for valid estimates of ZWD. A pressure error of 0.5 mb in the surface pressure measurement used to calculate the "hydrostatic term" of the tropospheric delay causes a 1 mm error in the zenith wet delay [6].

4. OTHER INSTRUMENTS

WWAVE included a number of other instruments to obtain PWV information for comparison with the GPS measurements. These other instruments, and the techniques used to obtain PWV from them, are described briefly.

4.1 SURFACE METEOROLOGY

The separation of the wet from the hydrostatic term of tropospheric delay requires accurate surface barometric pressure readings. Pressure sensors accurate to 0.5 mb were required for proper calibration of the WWAVE experiment. Two Paroscientific Barometers were used to calibrate the other barometers used in WWAVE listed in Table 1 in Section 5.

4.2 RADIOSONDE

Vaisala RS-80 Radiosondes were launched two or three times a day during daylight hours from a launch site at the parking lot of Haystack Observatory about 1 km north of the WVR location. The following specifications were provided by Vaisala. The Vaisala sondes measure the humidity with a thin film capacitor. Vaisala quotes a measuring range of 0 to 100% relative humidity (RH) with a resolution of 1% and a 1 s time lag. The humidity sensors have a reproducibility of better than 3% and a calibration repeatability of 2%. The pressure is measured with a capacitive aneroid sensor, with a measuring range from 1060 hPa to 3 hPa (mb), a resolution of 0.1 hPa, and an accuracy of 0.5 hPa both in the reproducibility and in the repeatability of calibration. The temperature is measured with a capacitive bead which has a measuring range from +60°C to -90°C, a resolution of 0.1°C, a reproducibility better than 0.4°C, and a repeatability of 0.2°C.

4.3 WATER VAPOR RADIOMETERS

A ground-based water vapor radiometer (WVR) is an instrument that scans the sky and measures the brightness temperature (radiation energy) of all water vapor along the line of sight. For WWAVE, a Radiometrics™ Corporation WVR-1100 portable water vapor radiometer was used. It operates at two frequencies. One channel is at 23.8 GHz, the other is at 31.4 GHz. The 23.8 GHz channel is dominated by water vapor but contains some cloud liquid signal, and the 31.4 GHz channel is dominated by cloud liquid, but contains some vapor signal. The contributions can be separated algebraically.

The WVR measures the sky brightness temperatures at the two frequencies and converts the measurements to atmospheric opacities. The WVR is calibrated using tipping curve measurements [15], an ambient blackbody target, and a noise diode. The radiometer output at each operating frequency is related to the atmospheric brightness temperature, T_b, which in turn is related to the absolute absorption τ (in nepers) by

$$T_b = 2.75e^{-\tau} + T_{mr}(1 - e^{-\tau}), \tag{6}$$

where T_{mr} is the mean radiating temperature of the atmosphere and T_{bg} is the cosmic background brightness temperature (both in Kelvins). The absorption at each frequency is derived from the measured T_b by

$$\tau_i = \ln\left\{\frac{T_{mr} - 2.75}{T_{mr} - T_i}\right\}, \tag{7}$$

where τ_i (i = 1,2) is the opacity at each of the two frequencies. T_{bg} has a value of 2.75 K.

Finally, PWV is derived from the absorptions at the two frequencies by

$$PWV = c_0 + c_1\tau_1 + c_2\tau_2, \tag{8}$$

where c_0, c_1, and c_2 are the values of the retrieval coefficients. The T_{mr} and retrieval coefficients were computed by linear regression analysis of the previous year's radiosonde data for July, August, and September from the NWS sites of Chatham, MA; Grey, ME; and Albany, NY. This analysis assumes a model for the molecular absorption of water vapor. Errors can be introduced in the determination of PWV through the retrieval algorithms, the absorption models for water vapor emission at the WVR frequencies, and/or the calibration uncertainties of the radiometer. It is estimated [16] that one can expect PWV retrieval biases of 1 mm PWV for dry conditions (6.5 mm zenith wet delay) and 2.5 mm of PWV (16-20 mm zenith wet delay) for very humid conditions.

4.4 VERY LONG BASELINE INTERFEROMETRY (VLBI)

VLBI is a technique which integrates important components of radio astronomy, atomic frequency standards, and high density data recording and data processing. VLBI observations are measurements of precisely time-tagged signals from extragalactic radio sources made simultaneously at a number of different radio telescopes. Hydrogen maser frequency standards are used to generate the precise time-tags of the observations. The cross-correlation of the VLBI data from the different stations allows for the calculation of both the difference in the arrival times of the signals and the rate of change of the

interferometric phase delay for each pair of telescopes. Typically, many different radio sources are observed (7 to 10 sources an hour) during observation periods of approximately 24 hours. By combining all of the VLBI delay and rate measurements, the relative positions of the radio telescopes and the radio sources can be determined. VLBI observations are used to support the production of regular, accurate determinations of Earth orientation parameters (polar motion, Universal Time, and nutation offset angles). They are also used to establish a reliable and consistent celestial and terrestrial reference frame, and are an important resource for geophysical studies of the Earth.

VLBI observations, and GPS measurements, are subject to atmospheric delay due to both the troposphere and the ionosphere. The ionospheric correction depends on the frequency that is observed. Typically, the radio sources observed during geodetic VLBI campaigns are at 2.3 and 8.4 GHz, frequencies that are much higher than either of the two GPS L-band frequencies. Thus, the ionospheric effects on the VLBI data are quite small. These effects are estimated using the two frequency data as is done in the GPS analysis. In the VLBI analysis, the tropospheric delay term is large with respect to other error sources. Many of the tropospheric recovery techniques used in GPS analysis were first developed within the VLBI community. Retrieval of the zenith wet delay from VLBI data is discussed in [17]. The basic procedure is the same as that used in the GPS analysis.

NASA sponsored the VLBI CONT95 campaign that took place during WWAVE. The radio telescopes that participated in CONT95 were the 20-m diameter antenna at Ny Alesund, Spitzbergen, Norway; the 18-m diameter antenna at Westford, MA, USA; the 26-m diameter antenna at Gilmore Creek, Fairbanks, AK, USA; the 20-m diameter antenna at Onsala, Sweden; the 20-m diameter antenna at Kokee, HI, USA; and the 20-m diameter antenna at Wettzell, Germany.

5. THE EXPERIMENT

The Westford Water Vapor Experiment (WWAVE) took place from 8 August to 12 September 1995. The main dates for WWAVE were chosen to coincide with the NASA sponsored CONT95 VLBI campaign, which took place from 15-29 August 1995. Five types of data were collected: surface meteorological, radiosonde, water vapor radiometer (WVR), very long baseline interferometry (VLBI), and GPS data. The surface meteorological data consisted of either surface pressure, temperature, and humidity measurements, or simply surface pressure measurements. The surface pressure data were used to separate the GPS estimate of the tropospheric wet delay from the total tropospheric delay. The radiosonde launches consisted of balloons carrying Vaisala sonde packages with pressure, temperature, and humidity sensors. The radiosondes were launched twice daily from the Haystack Observatory parking lot, a location close to three of the GPS receivers, and also the location of the WVR. Radiosonde data were also collected from the twice daily launches by the National Weather Service at Chatham, MA; Grey, ME; and Albany, NY. The National Weather Service uses Viz sonde packages. Finally, a single additional launch (also using a Vaisala sonde package) from the Phillips Lab on the Hanscom AFB near Lincoln Laboratory was used to verify the data processing of the Haystack radiosonde data. The WVR was positioned approximately 200 meters from the northernmost of the three Westford GPS sites (MHR0) and approximately 625 m from the radiosonde launch site.

The water vapor radiometer data were collected continuously from 8 August through 12 September 1995. A radiosonde was launched twice daily from the Haystack Observatory parking lot starting 15 August and continuing through 29 August. The GPS data collection period began 15 August and extended through 5 September 1995.

Table 1 gives the details of the various GPS receivers used in the WWAVE experiment and of their corresponding weather stations. The relative positions of the various GPS receivers are indicated on the map shown in Figure 1.

A primary goal of this report is to assess the accuracy of the GPS estimates of the zenith wet delay (which can be converted to precipitable water vapor). Therefore, the majority of the GPS data presented were taken from the three closely related GPS sites, WES2, WFRD, and MHR0, which are represented by the three stars in the center of Figure 1. The WVR at the Firepond facility and the Haystack radiosonde launches were also located near the position of the top of these three stars in the center of the circle. The spacing of the symbols is not indicative of the actual separation of the antennas. Note also the location of the two Ashtech receivers with the Dorne-Margolin antennas: ULWL and NVT0. NVT0 is located further south of the ULWL site in between the town centers of Westford and Chelmsford, about 10 km from the center location of Haystack.

TABLE 1

Westford Water Vapor Experiment: GPS Receivers

SITE	LOCATION	RECEIVER	ANTENNA
MHR0 *	Millstone Radar Pole on Roof Westford, MA	AOA Turbo Rogue	Dorne-Margolin with choke ring
WES2 *	Westford Antenna 10 m Tower Westford, MA	AOA Turbo Rogue	Dorne-Margolin with choke ring
G420 **	Lincoln Lab Pole on Flat Roof Hanscom AFB, MA	AOA Turbo Rogue	Dorne-Margolin with choke ring
WFRD *	Ground Mount Westford, MA	AOA Turbo Rogue	Dorne-Margolin with choke ring
AEN0 ***	Tripod on Peaked Roof Harvard, MA	AOA Turbo Rogue	Dorne-Margolin with choke ring
ULWL **	University of Lowell Tripod on Flat Roof Lowell, MA	Ashtech Z-12	Ashtech 700936B Dorne-Margolin choke ring & radome
NVT0	Nashoba Tech High School Tripod on Flat Roof Westford, MA	Ashtech Z-12	Ashtech 700936B Dorne-Margolin choke ring & radome
SGJ0 ***	Tripod on Peaked Roof Pepperell, MA	AOA Turbo Rogue	Dorne-Margolin with choke ring
JIM1	Ham Radio Tower Dunstable, MA	Ashtech Z-12	Ashtech 700718B Surveying Antenna
FIRE	Groton, MA Pepperell, MA	Ashtech Z-12	Ashtech 700718B Surveying Antenna
TAC0 *	Tripod on Peaked Roof Nashua, NH	AOA Turbo Rogue	Dorne-Margolin with choke ring

* Rainwise Weather Station
** Vaisala Weather Station
*** Paroscientific Barometer

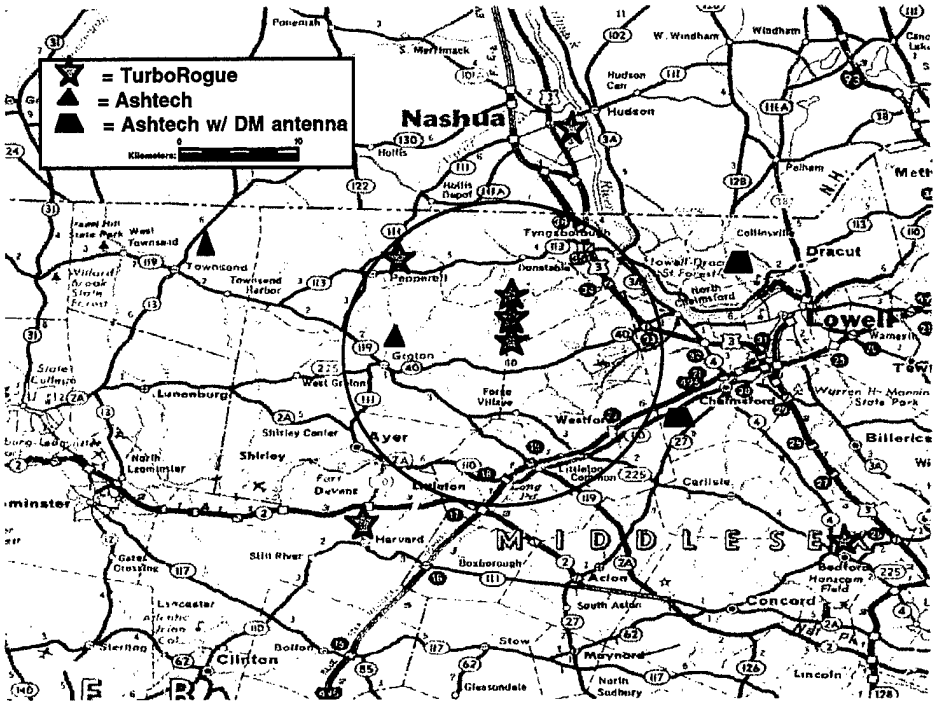

Figure 1. Map showing location of the GPS receiver sites.

The GPS derived positions in the WGS-84 coordinate frame at ten of the GPS sites are given in Table 2. These positions were derived using an average of the GPS data over the 15 days of the main experiment (Day 230-244). The positions have a precision on the order of 5 mm. Approximate positions are also listed for the Westford VLBI antenna, the WVR, and the radiosonde launch site at Haystack Observatory. Note the difference in heights between the different stations.

TABLE 2

WGS-84 Positions of Primary GPS Sites and of the WVR and Radiosonde Launch Sites

	Latitude (deg)	E. Longitude (deg)	Height (m)
MHR0	42.617896	288.508854	112.8
WFRD	42.608159	288.505986	56.4
WES2	42.613338	288.506674	85.2
AEN0	42.528733	288.444811	99.1
G420	42.459498	288.734843	54.8
JIM1	42.639783	288.312330	86.1
FIRE	42.610088	288.442356	146.4
SGJ0	42.665783	288.443781	43.0
ULWL	42.654521	288.674082	23.5
NVT0	42.571037	288.590345	65.4
VLBI* Westford	42.62	28.5	116
WVR*	42.618	288.51	107
Haystack Radiosonde*	42.623	288.51	92

*approximate positions

Figure 2 shows the relative location of the Haystack radiosonde launch site, the MHR0 GPS site, and the WVR site at the central location of the Haystack/Millstone complex. The other two GPS locations at the central site are located further down the hill (the bottom of the photograph) and are not shown in Figure 2.

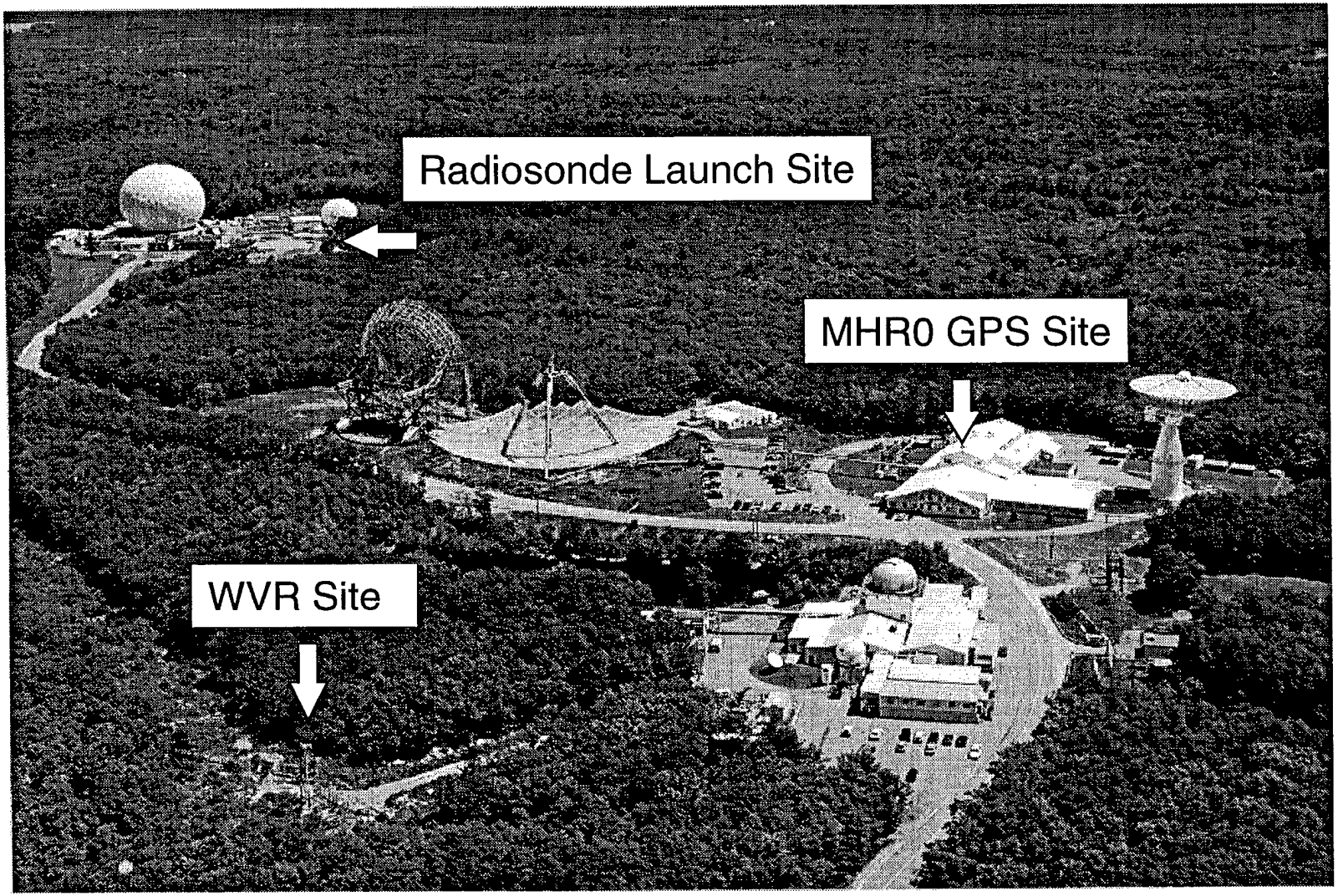

Figure 2. The relative locations of the Haystack radiosonde launch site, the MHR0 GPS site, and the WVR site.

6. DATA ANALYSIS

This section focuses on the comparisons of the different kinds of data. First, a comparison is made between the zenith wet delays measured by the Haystack radiosonde launches and those measured by the three closest NWS radiosonde sites in Grey, ME; Chatham, MA; and Albany, NY. Following this, a comparison between the Haystack radiosonde derived zenith wet delays and the WVR determined zenith wet delays is shown for the 15 day period of the main experiment. The estimated zenith wet delay associated with the nearest GPS site to both the WVR location and to the Haystack radiosonde launch site is then added to the radiosonde and WVR comparison. Finally, the VLBI estimates of zenith wet delay are compared to those from the WVR, GPS, and Haystack radiosonde. As a further test of GPS self-consistency in retrieving ZWD, data from three closely spaced GPS sites are compared for the 15 day time period. This analysis allows an assessment of the accuracies offered by the different kinds of techniques used to measure precipitable water vapor, including an analysis of GPS antenna and receiver issues that can bias the ZWD retrieval.

6.1 COMPARISON OF THE HAYSTACK RADIOSONDE AND THE NWS RADIOSONDE ZENITH WET DELAY

Figure 3 shows the zenith wet delays calculated from the Haystack radiosonde data and the NWS radiosonde data from Chatham, MA; Grey, ME; and Albany, NY. The zenith wet delays were calculated using a raytrace program [10] which computes the zenith wet delay from the pressure, temperature, and relative humidity. What is clearly evident in Figure 3 is that the Haystack estimates of zenith wet delay are consistently lower than the other three NWS sites. On average the difference is 36 mm in zenith wet delay. Although these sites are approximately 150 km away, since Haystack is in the center of the region (east of Albany, NY, and west of Chatham, MA, and Grey, ME), the consistently lower value measured for zenith wet delay indicated a possible problem. The average differences in estimated zenith wet delays obtained from the NWS sondes and the Haystack sondes are summarized in Table 3.

The Chatham (CHH) and Grey (GYX) measurements of zenith wet delay might be expected to be slightly larger than the Haystack (HST) values since these sites are located near the ocean and are at lower altitudes. However, the consistently larger average value of precipitable water vapor seen at Albany (ALB) was surprising. Closer evaluation of these discrepancies indicated that the differences could be partly attributed to the different type of sondes and data processing algorithms used. The VIZ sondes of the National Weather Service (NWS) use hygristors to measure the humidity, and it is known that hygristors are less accurate in regions of very high or very low humidity. In fact, the weather service does not report relative humidities below 20% RH [18], [19]. The Vaisala sondes used during the Haystack launches typically measure drier than the VIZ sondes. The NWS is in the process of converting over to Vaisala sondes. To verify our data processing, a Haystack Vaisala sonde data set (HST) was

compared with a data set from another Vaisala sonde flown simultaneously from Phillips Laboratory on Hanscom AFB (HAN) located approximately 25 km from Haystack [20]. The resulting humidity profiles agree to 3% from 1000 to 50 mb except for a feature from 800 to 700 mb, which differed by 10%. Figure 4 shows the humidity profiles generated by the HAN, HAY, ALB, CHH, and GYX sondes launched 1995 August 25 at 1200 UT (DOY 237.5).

TABLE 3

The Average Differences in Zenith Wet Delay Between the Albany, Chatham, Grey, and Haystack Radiosondes

	Average Difference in ZWD (mm)	Std. Dev.of the Diff. in ZWD (mm)
ALB-HST	+35 (6 PWV)	27 (4 PWV)
CHH-HST	+46 (8 PWV)	41 (7 PWV)
GYX-HST	+19 (3 PWV)	24 (4 PWV)

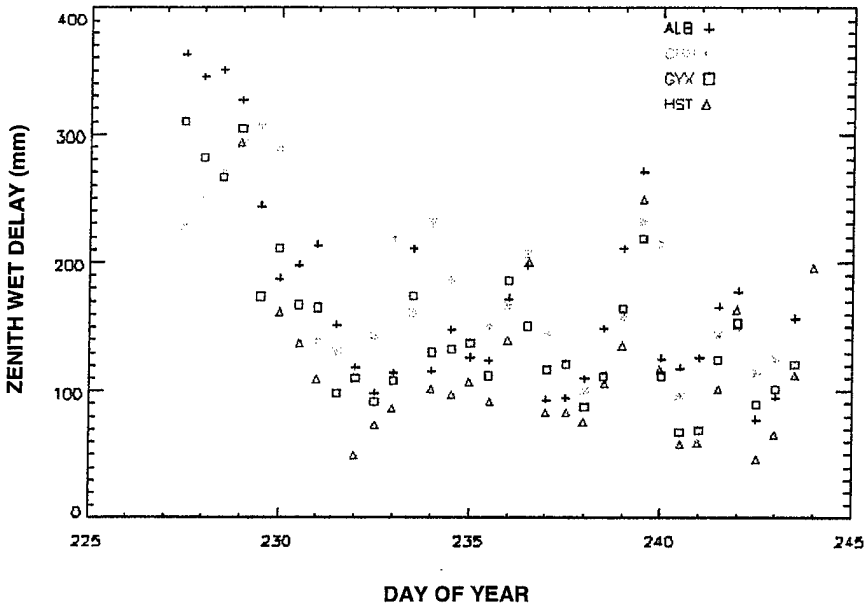

Figure 3. Zenith Wet Delays calculated from NWS radiosonde data launched from Albany, NY; Chatham, MA; and Grey, ME, and from the Haystack radiosonde data.

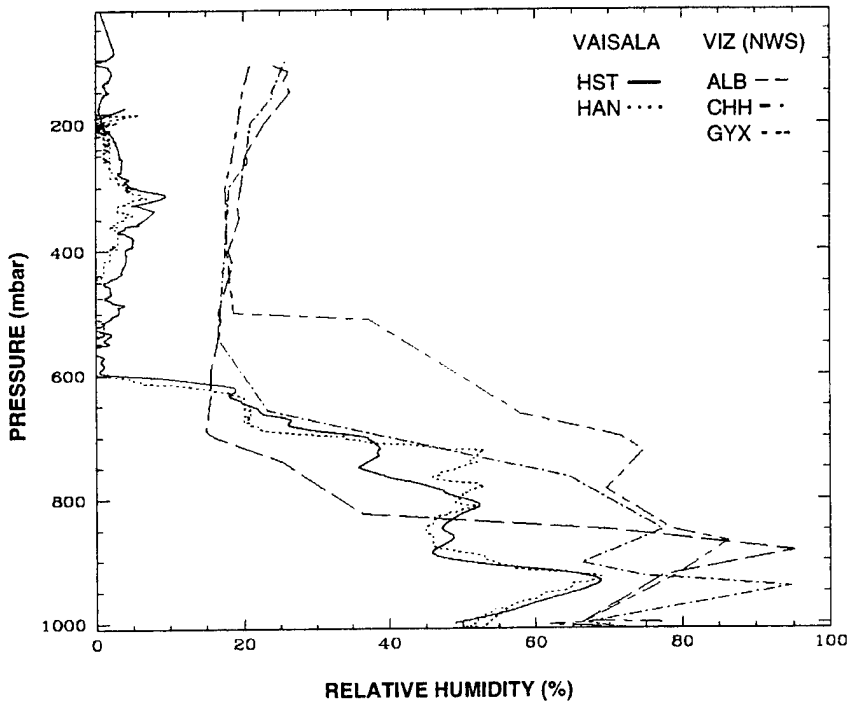

Figure 4. The relative humidity--pressure relation for radiosondes launched 1995 August 25 1200 UT for the three NWS sites (VIZ sondes) nearest Haystack Observatory and for Vaisala sondes launched at Haystack Observatory and at Phillips Laboratory.

6.2 COMPARISON OF THE HAYSTACK RADIOSONDE AND THE WVR ZENITH WET DELAY

Figure 5 shows both WVR estimates of zenith wet delay and Haystack radiosonde estimates. The liquid water scale is given on the right hand abscissa. Evidence of rain is apparent in the small peaks in the liquid water on Days 236, 239 and 244. The WVR data reflects the amount of PWV directly above the WVR at Haystack. The WVR was scanning in both elevation and azimuth, but the data shown here correspond to the measurements made at 90 degrees elevation only. The WVR beamwidth at 90 degrees elevation is about 5.5 degrees [21]. An additional comparison was made between the radiosonde data and a second set of WVR data. This second set estimated the ZWD by using the Neill wet mapping function [10] to translate the WVR scans at 14, 19, 27, 45, and 90 degrees elevation to zenith. There was no statistical difference in the comparisons between the two WVR data sets and the radiosonde data.

Excluding the WVR data associated with rain, evident in the graph on Days 236, 239, and 244, the average difference between estimated zenith wet delays obtained from the WVR and from the Haystack radiosonde launches is +18.3 mm with a standard deviation of 12.5 mm. Liquid water on the WVR in the

ray path direction (for example, on the cover of the unit) may cause erroneous readings of the path delay. For this reason, these data were excluded.

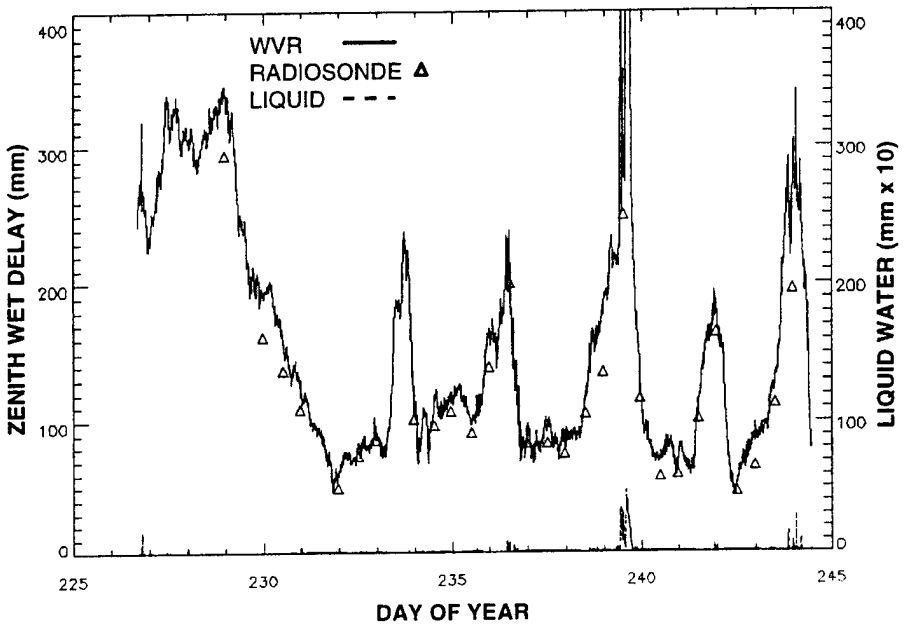

Figure 5. Difference between the WVR and Haystack radiosonde estimates of the Zenith Wet Delay.

The average measured difference between the Haystack radiosonde estimate and the WVR estimate of zenith wet delay is equivalent to about 3 mm of difference in precipitable water vapor. It is worth noting that the retrieval coefficients used for the WVR used in WWAVE were derived using an average of three months of NWS radiosonde data (presumably VIZ sondes) for this time period from the previous year. The WVR retrieval coefficients should be re-estimated using the Haystack radiosonde data or other data taken with Vaisala sondes. Unfortunately, retrieval coefficients based on the Haystack Vaisala data alone would have large uncertainties due to the small amount of data.

6.3 COMPARISON OF RADIOSONDE, WVR, AND GPS ZENITH WET DELAY

Estimates of the ZWD from the WVR and from the MHR0 GPS receiver during the experiment are shown in Figure 6. MHR0 is the receiver located closest both to the WVR location (about 200 m away and 6 m higher) and to the Haystack parking lot where the radiosondes were launched (about 625 m away and 20 m higher). The locations of these three sites are given in Table 2.

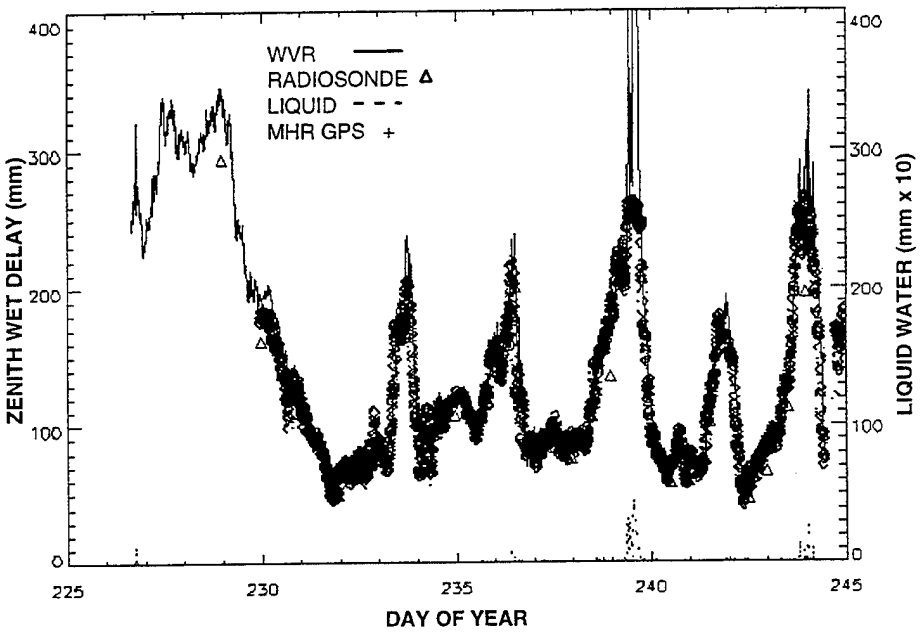

Figure 6. Estimates of Zenith Wet Delay by WVR, radiosonde, and GPS.

The average difference between WVR and GPS estimated zenith wet delays (again excluding time periods associated with rain) was +6 mm with a standard deviation of 9 mm. Time periods associated with rain were defined to be those with a measured delay due to liquid water greater than 0.3 mm. The average difference between GPS and radiosonde estimated ZWD was +12 mm with a standard deviation of 14 mm.

6.4 COMPARISON OF RADIOSONDE, WVR, AND VLBI ESTIMATES OF ZENITH WET DELAY

Estimates of the ZWD from a partial segment of the VLBI campaign [22] are shown in Figure 7. The position of the Westford antenna used in the VLBI campaign is given in Table 2. The GPS estimates of ZWD were not plotted here since visually they cannot be separated from the VLBI estimates.

The statistical analysis of the four data sets, VLBI, GPS, WVR, and radiosonde, shows that VLBI estimates of ZWD are, on average, larger than the estimates of all the other measuring techniques. These results are summarized in Table 4. The average difference between VLBI and WVR estimated zenith wet delays (excluding the time periods associated with rain) was +3 mm. The average difference between VLBI and GPS estimates of ZWD was +8 mm, and the average difference between VLBI and radiosonde estimates was +24 mm.

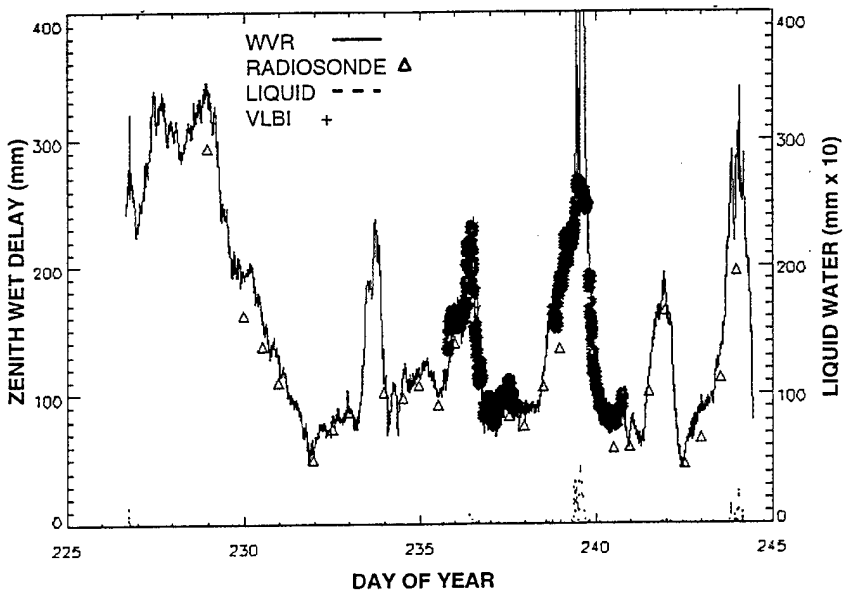

Figure 7. Estimates of Zenith Wet Delay by WVR, radiosonde, and VLBI.

TABLE 4

Average Difference and Standard Deviation in the Zenith Wet Delay Estimated by WVR, Radiosondes, and GPS

	Ave. Diff. In ZWD (mm)	Std. Dev. In Diff. Of ZWD (mm)
WVR – GPS	+6 (1 PWV)	9 (1.5 PWV)
GPS – Radiosonde	+12 (2 PWV)	14 (2 PWV)
WVR – Radiosonde	+18 (3 PWV)	13 (2 PWV)
VLBI – GPS	+8 (1.5 PWV)	10 (1.5 PWV)
VLBI – WVR	+3 (0.5 PWV)	9 (1.5 PWV)
VLBI – Radiosonde	+24 (4 PWV)	11 (2 PWV)

The difference between GPS and WVR estimates of ZWD is illustrated in Figure 8. The data in this figure show that, aside from an average offset of 4.4 mm between GPS and WVR estimates of ZWD, there is no obvious departure from a linear fit between the two data sets.

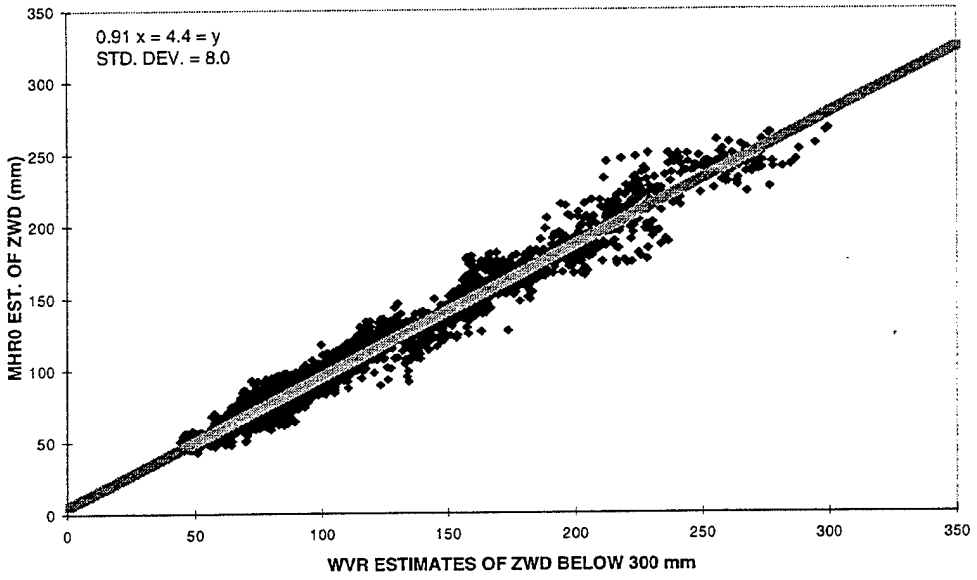

Figure 8. Scatter plot of the WVR and GPS estimates of Zenith Wet Delay.

6.5 COMPARISON OF THE GPS DERIVED ZENITH WET DELAYS AT THREE SITES FOR DAYS 230-244

Figure 9 shows the zenith wet delays estimated by the three closely spaced GPS receivers, MHR0, WES2, and WFRD. All of these data were taken with AOA Turbo Rogue GPS receivers with Dorne-Margolin antennas with choke rings. Note the nearly identical structure observed by all three sites.

The average differences between the zenith wet delays at the three sites are given in Table 5. These differences may be due to some combination of real differences in water vapor at the three sites, error in the barometer value used to remove the hydrostatic components, or systematic errors associated with the electromagnetic environment of the antenna. The difference in the heights of the three stations alone would require corrections of –1.4 mm, –1.4 mm, and –2.8 mm for the three rows of Table 5, given a uniform distribution of water vapor up to a height of 3000 m and an average ZWD of 150 mm.

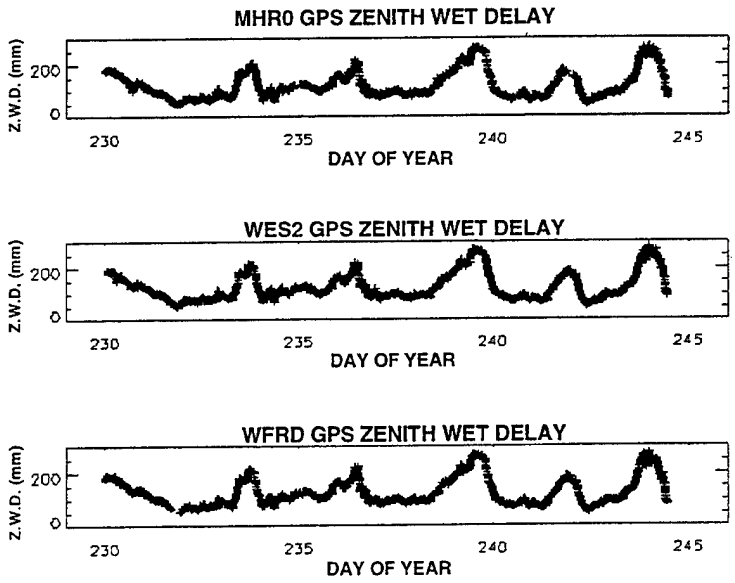

Figure 9. GPS estimates of the Zenith Wet Delay for three sites from Day 230 to Day 244, 1995.

TABLE 5

Average Difference Between GPS Derived Zenith Wet Delay at Three Sites for Days 230-244

	Mean Difference in ZWD (mm)	Std. Dev. of Difference in ZWD (mm)	Height Diff. Of Sites (m)
WES2-MHR0	+4.4 (0.7 PWV)	6.2 (1.0 PWV)	-27.5
WFRD-WES2	+1.2 (0.2 PWV)	4.8 (0.7 PWV)	-28.8
WFRD-MHR0	+5.5 (0.8 PWV)	6.8 (1.0 PWV)	-56.3

The ZWD data estimated from the three closely spaced receivers were plotted, grouping the sites in pairs. A linear regression was performed in each case. The plots are shown below in Figures 10a, b, and c.

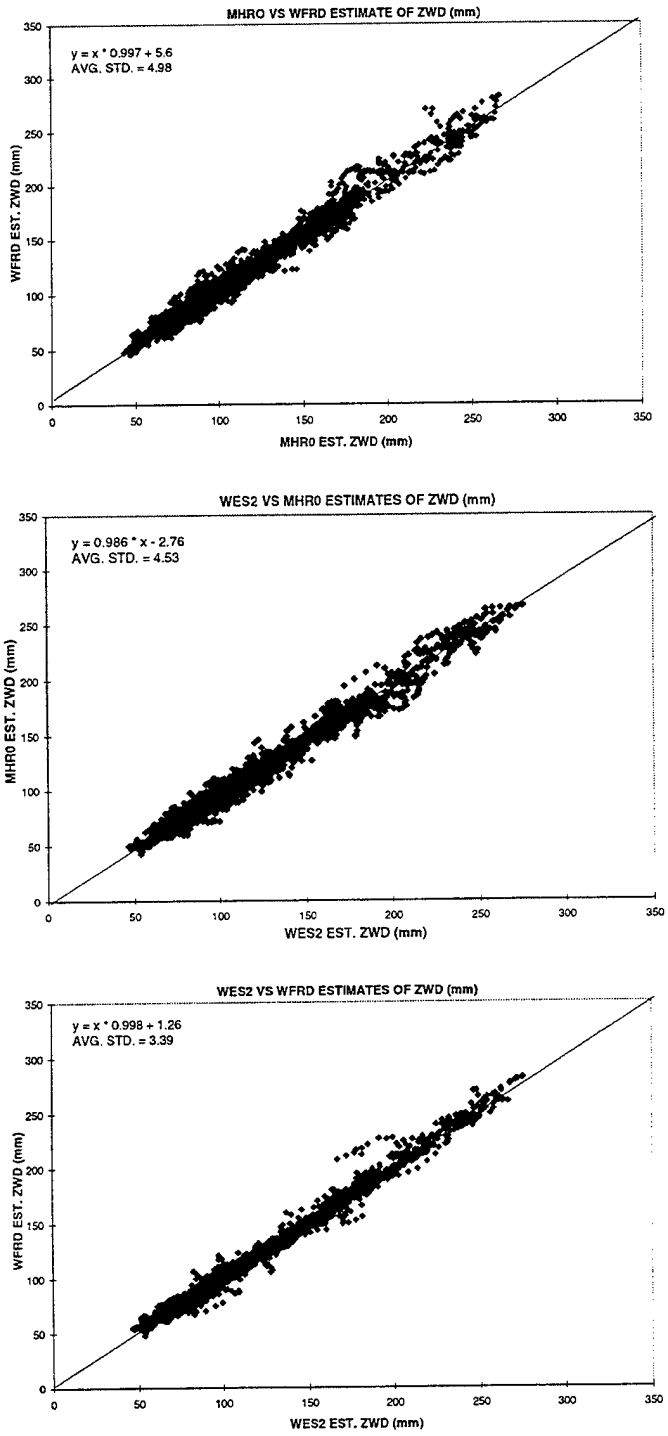

Figures 10a,b,c. Scatter plots of Zenith Wet Delay estimates between a) MHR0 and WFRD, b) WES2 and MHR0, and c) WES2 and WFRD GPS receivers.

The overall scatter (average standard deviation about the line of best fit) is the smallest between the WES2 and WFRD sites (Figure 10c) which are the two physically closest sites. The anomalous scatter between WES2 and WFRD, evident in Figure 10c (the line of higher PWV values at about 175 to 200 mm of ZWD), corresponds to the time period 244.25 - 244.37. This same anomalous scatter also exists between the other sites (Figures 10a and 10b), although it is not as visually apparent. This time period is discussed in more detail in the next section.

It is doubtful that errors in pressure caused the average difference in PWV estimates at the three sites. Pressure gradients observed during the WWAVE experiment were shown to be, on average, negligible based on a comparison of the barometer differences from the various sites. Pressure measurements from the Rainwise barometer at the MHR0 site were used to compute the pressures at the antennas for MHR0, WES2, and WFRD using the height differences. This barometer was calibrated on two occasions during WWAVE against a Paroscientific barometer, which has an advertised accuracy of better than 0.1 mb.

If one assumes roughly 0.05 mm of ZWD per meter near the surface of the earth, the difference in height between WFRD and MHR0 (56 m) could partially account for the average difference in their measured ZWD. The observed ZWD differences in Table 5 do increase with height difference but are not consistent with a uniform layer of water vapor (note the differences between WES2-MHR0 and WFRD-WES2). Possible physical differences in the environment, such as the presence of trees around the WES2 site, might account for some of the discrepancy in the average ZWD differences between the sites. The WFRD site is located in a fairly flat grass covered field. The antenna for WES2 is mounted on top of a 10 meter steel tower. The tower is surrounded by trees. The MHR0 antenna is mounted on the roof of the main Millstone Radar building, surrounded by a parking lot, with no vegetation close by. One could therefore anticipate slightly "drier" readings of PWV at the MHR0 site, which is consistent with the data in Table 5.

It is also likely that some of the differences seen in the estimated zenith wet delay can be attributed to the different antenna mounting configurations used. Niell, et al., (1996) found systematic differences of up to 3 mm in ZWD for Turbo Rogue Dorne-Margolin antennas separated by only 15 m when analyzed with a 5° elevation cutoff. The only differences in the receivers and antennas were the mount and the use of a radome. In that study, two antennas were placed on tripods near the WFRD site, while the WFRD antenna was located on a concrete pillar and covered by a radome. Both the radome and the concrete pillar mount were shown to influence estimates of ZWD. Antenna mounts are discussed in more detail in Section 7.2.

6.6 EVIDENCE OF SMALL SCALE VARIATIONS IN PWV

One of the more exciting aspects of using GPS to monitor PWV is the concept that GPS will provide a new window with which to watch the development and propagation of weather fronts.

Although no major weather pattern developed during WWAVE, it did rain twice during the experiment: on Day 239 and again on Day 243 into Day 244. The zenith wet delays associated with the beginning of Day 244 showed evidence of a wave-like pattern superimposed on the relatively high value of the zenith wet delay. This pattern was evident in the estimated zenith wet delays from all of the GPS sites analyzed that day but not for other days. Figure 11 shows the data from the two most separated sites with AOA Turbo Rogue receivers: GR42, which is the site furthest to the east on Hanscom AFB in Lexington, MA, and AEN0, which is the site located furthest to the west in Harvard, MA (see Figure 1). The sites are separated by approximately 40 km. In the middle third of the day it is clear that the change in water vapor content at GR42 lags that at AEN0, which is consistent with both the general west-to-east weather pattern in this area and the prevailing westerly winds on that day as seen in NWS radiosonde data.

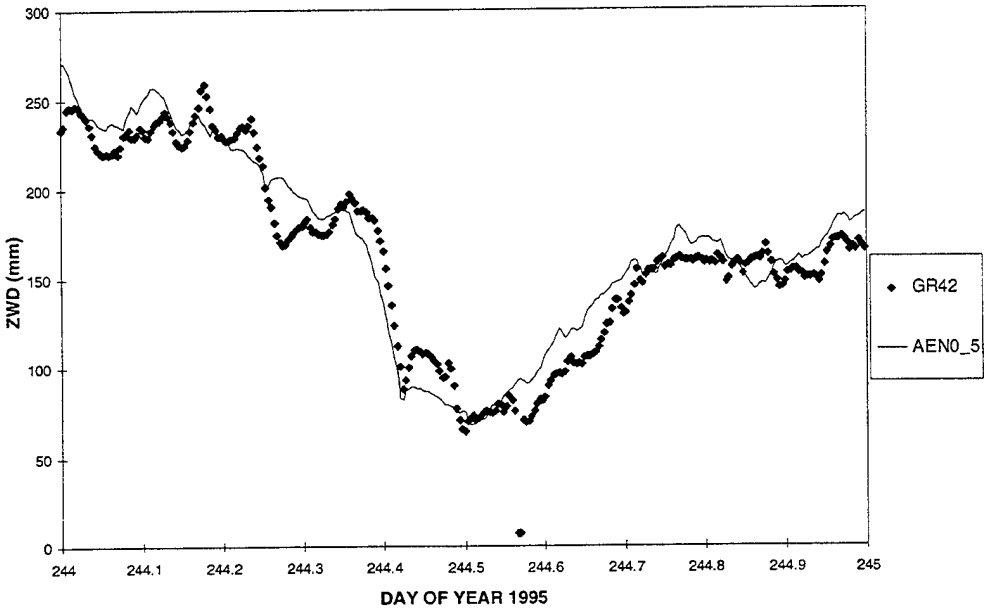

Figure 11. Estimated Zenith Wet Delays from two separated sites.

The wave-like structures can also be observed in the GPS estimated ZWD data from the three closely located sites at the Millstone/Haystack complex shown in Figure 12. Recall that the anomalous PWV data seen in Figure 10c was observed between 244.25 and 244.37. A clear separation of ZWD estimates can be observed at the three sites during this time period.

The final plot in this section, Figure 13, shows the difference between the GPS estimated ZWD at MHR0 and the WVR estimate of ZWD during this same time period on Day 244. The WVR determined liquid water vapor content is also shown and is scaled according to the information given on the right-hand axis of the graph. Note that the same wave-like structure in the ZWD is observed in the WVR data.

This suggests that this was a real phenomenon rather than some obscure artifact of the GPS data processing.

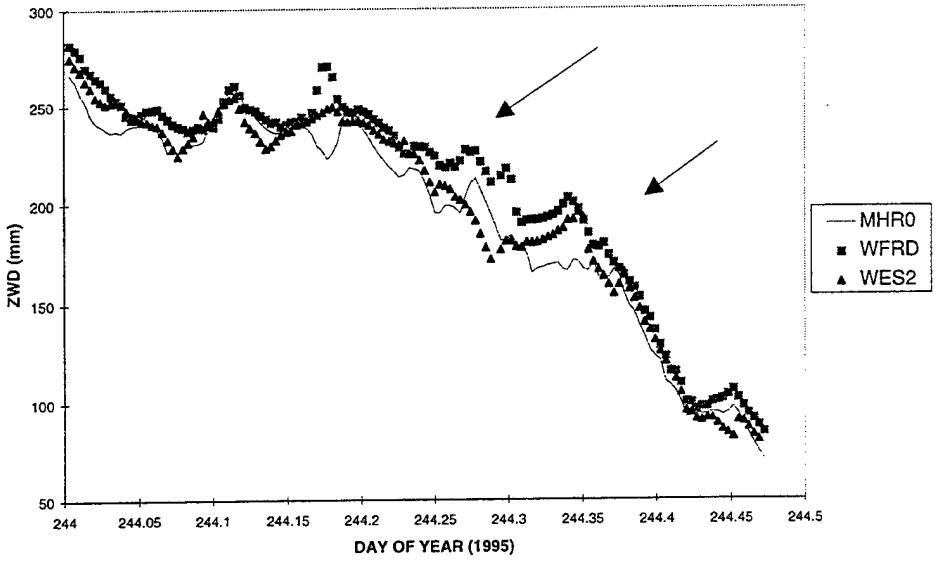

Figure 12. Anomalous Zenith Wet Delay estimates between the three closely located GPS sites: MHR0, WES2, and WFRD on Day 244.

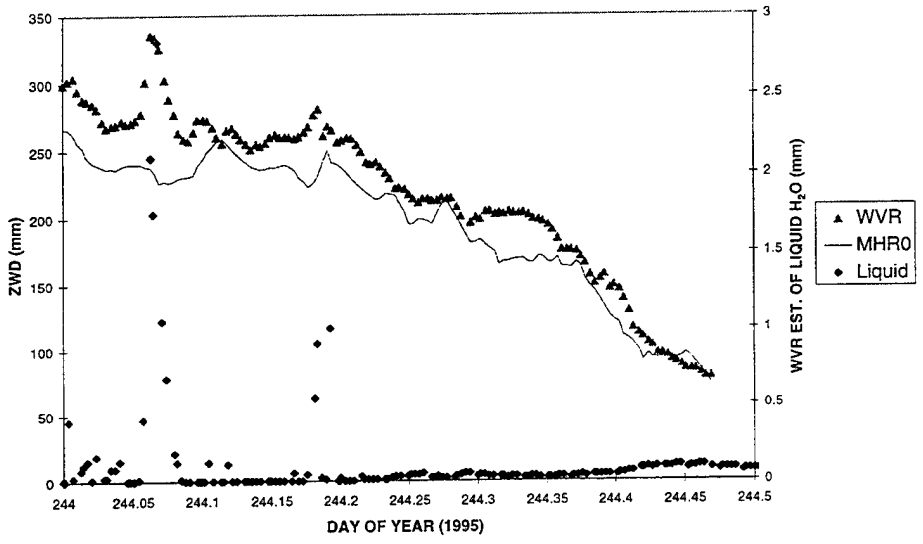

Figure 13. GPS estimates of Zenith Wet Delay versus WVR estimates of ZWD on Day 244.

7. REAL-TIME CONSIDERATIONS

A secondary goal of WWAVE was to examine issues related to the real-time determination of PWV. A brief summary of the work being done by other groups will be presented. This section focuses on the effect of different types of GPS receivers, and GPS antennas and antenna mounts, on the retrieval process of PWV. To this end, different types of GPS receivers and antennas were compared during this campaign. An analysis of the effect of different elevation cutoffs of GPS data used in solving for the PWV is presented. In addition, a comparison of the ionospheric delay term using data from the two different types of receivers (AOA Turbo Rogue and Ashtech Z12) is shown. While determination of the ionospheric delay is not directly related to the PWV measurement in GPS, it must be correctly accounted for, and an error in its determination will influence the PWV estimate. With the advent of anti-spoofing, the real-time determination of this quantity has been affected and needs to be considered in some detail.

7.1 REAL-TIME DETERMINATION OF PWV

The real-time, or near real-time, determination of water vapor from GPS data depends on the ability to either determine the various sources of error in GPS estimation, or to eliminate them by double and single differencing. These factors include the satellite orbits, the satellite clock offsets, and the ionospheric correction term. For the past few years, ERL, the Environmental Research Laboratories of the National Oceanic and Atmospheric Administration, has had an ongoing project to demonstrate the capability of monitoring the atmospheric water vapor in real-time using GPS signal delays and to implement this capability within NOAA. As noted, the key to near real-time determination of PWV is the determination of the precise GPS satellite orbits. Several groups are now claiming to be able to predict accurate near real-time GPS orbits, including JPL and Scripps Institute of Oceanography [24].

Since June 1996, the UNAVCO GPS Research Group has been analyzing GPS data from the NOAA Forecast Systems Laboratory (FSL) network to provide real-time hourly PWV estimates. Chris Rocken's web site (www.unavco.ucar.edu/~rocken) has a description of their work, displays of their near real-time PWV estimates, and plots of the long term comparison of these estimates. This analysis has been on an experimental basis using data from a 12 receiver network in Colorado, Kansas, Oklahoma, New Mexico, Arkansas, and Mississippi. The receivers are dual frequency Trimble 4000 SSE instruments with Trimble SSE antennas. The near real-time PWV data shown at Rocken's web site can be in error by as much as 8 mm in PWV (50 mm of zenith wet delay) when compared to the post-processed data. In particular, the sites in Oklahoma show WVR and radiosonde estimates of PWV for comparison with both the near real-time GPS estimate of PWV and the final GPS estimate of PWV. It should be pointed out that this real-time analysis is still in a preliminary stage, and that their results are experimental only. However, it is these accuracy issues that this section will address.

In the following sections, the issues of both elevation cutoff dependence and receiver type are examined. Both of these issues are critical to a rapid, accurate determination of PWV.

7.2 ELEVATION CUTOFF DEPENDENCE

One of the goals of WWAVE was to examine the effect of different types of antennas and antenna mounts on the retrieval of PWV. The retrieval of PWV, especially in a near real-time scenario, depends on the separation of the tropospheric delay term from other estimated quantities, such as satellite and receiver clock biases. High quality low elevation data are extremely useful in determining all of the unknown quantities in the GPS data. However, with the advent of anti-spoofing, the deliberate policy of the DoD to corrupt the GPS performance, the signal-to-noise ratios of the low elevation data have been significantly degraded. With some receivers, this effect is worse than others.

In an attempt to examine this issue, the retrieval of GPS-determined ZWD as a function of elevation was compared for ten different sites during the WWAVE experiment: WES2, WFRD, MHR0, SGJ0, G430, AEN0, FIRE, ULWL, NVT0, and JIM1. With the exception of FIRE, ULWL, NVT0, and JIM1, all of the data examined were taken with AOA Turbo Rogue receivers and Dorne-Margolin choke ring antennas. The FIRE and JIM1 sites used an Ashtech Z-12 receiver and the standard Ashtech surveying antenna, the 700718B. The NVT0 and ULWL sites used an Ashtech Z-12 antenna with a Dorne-Margolin choke ring antenna and a radome, the 700936B.

Estimates of the ZWD for each site were determined using elevation cutoffs of 5, 10, 15, 20, 25, and 30 degrees. The elevation cutoff merely represents the elevation below which GPS data were excluded from the estimation procedure for ZWD. Once these estimates were obtained, the average difference between the ZWD estimate for the elevation cutoff being examined and the ZWD estimate for that site using a 5 degree cutoff was computed, i.e., ZWD(elcutoff) - ZWD(5°). This set of differences for all of the GPS sites is plotted in Figure 14 as a function of the elevation cutoff. The data in Figure 14 are the averaged differences over Day 236 during WWAVE. The 5° elevation cutoff represents the zero point, since all other elevations are differenced to that value. The best antennas and antenna configuration should show little or no dependence on elevation cutoff.

What is extremely evident in Figure 14 is that two of the sites, FIRE and JIM1, show a very strong dependence on elevation cutoff. These sites both use an Ashtech Z12 receiver with an Ashtech 700718B antenna. The FIRE antenna was mounted above a flat metal roof on a building atop the Groton fire tower. The antenna at the JIM1 site was located on top of a 13 m amateur radio tower. Both sites show very similar elevation dependence at all elevations. This suggests that the extreme elevation dependence (80 mm in ZWD difference) is dominated by the antenna and not the mount. This standard surveying antenna does not have the multi-path rejection capability offered by the Dorne-Margolin choke ring antenna, and is known to also have a large intrinsic elevation dependent phase error for which no correction has been made.

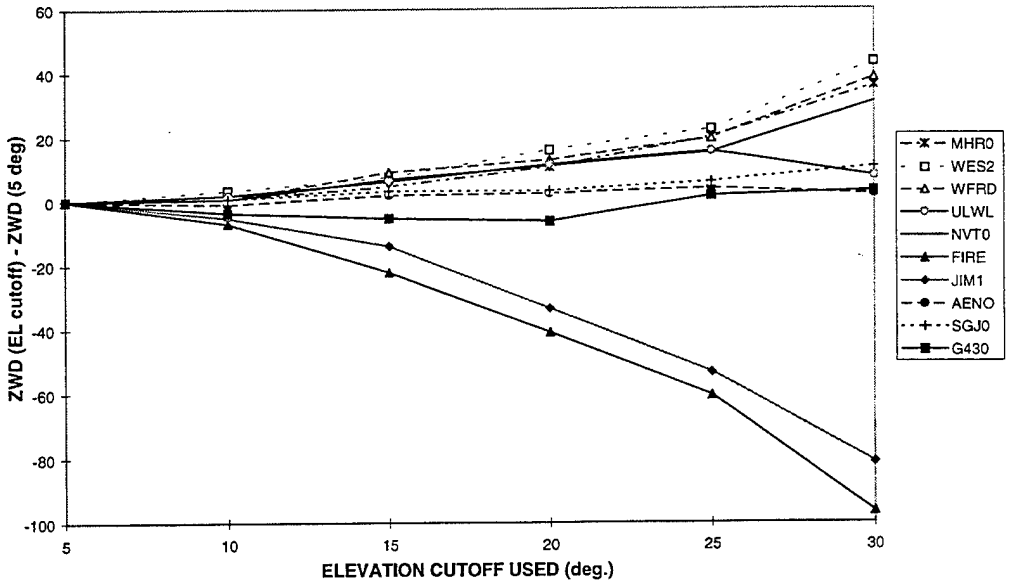

Figure 14. Elevation cutoff comparison between sites.

Figure 15 shows the performance of GPS receivers at the ULWL and NVT0 sites. Both of these sites used the Ashtech Z-12 receiver with a Dorne-Margolin choke ring antenna with a radome. The

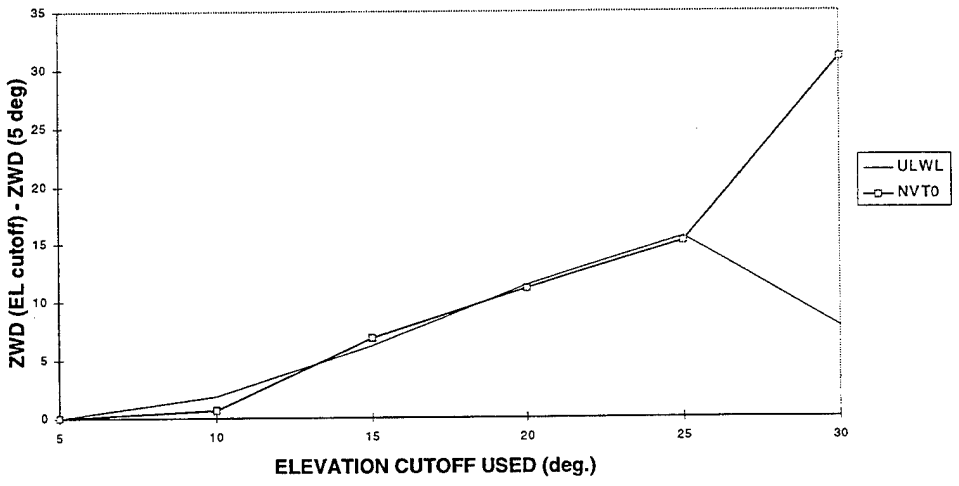

Figure 15. Elevation cutoff comparison with the Ashtech Z12 receivers with the Dorne-Margolin choke ring antennas with radome.

difference between the 5° and 10° cutoff is minimal. The two sites are separated by almost 10 km, so it is worth noting that the dependence on elevation cutoff is almost identical up until the 25° elevation cutoff point. It is possible that this may be partially attributed to the influence of radome. The Ashtech Dorne-Margolin antennas have radomes which have been shown to influence the determination of PWV as a function of elevation [23].

Figure 16 shows the elevation cutoff dependence of the six sites equipped with AOA Turbo Rogue GPS receivers and Dorne-Margolin antennas. These sites were WES2, WFRD, MHR0, AEN0, SGJ0, and G420. There is a clear division illustrated in Figure 16. Three of the sites show little or no elevation cutoff dependence, AEN0, SGJ0, and G420, while the other three sites show a dependence on elevation cutoff on the order of 36 mm in ZWD (6 mm in PWV). Two of the best sites, AENO and SGJ0, had antennas that were standard tripod/tribach mounts and were installed on the peak of asphalt roofs. The other site that showed good performance was at G420. Here the antenna was mounted on a wooden platform about 30 cm above a flat rubberized roof.

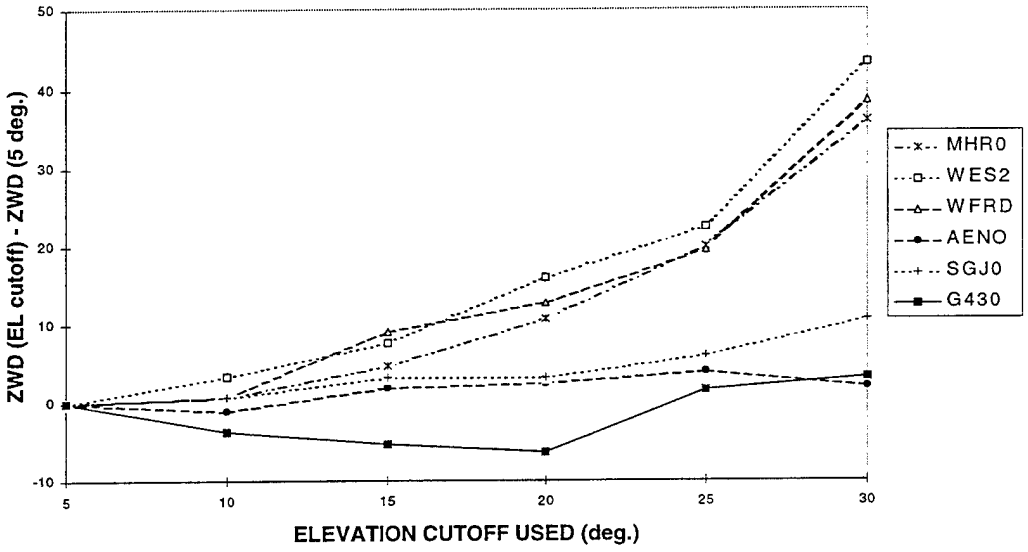

Figure 16. Elevation cutoff comparison AOA Turbo Rogue GPS receivers with Dorne-Margolin antennas.

The antennas at WES2, WFRD, and MHR0 sites were mounted in various configurations. WFRD was located in a fairly flat open field. The antenna for WFRD was mounted in an aluminum ring with the bottom of the choke rings 96 mm above the surface of a 0.76 m diameter concrete pillar. The surface is ~1 m above the ground and is inlaid with a plate 0.46 m in diameter which contains the geodetic reference mark for the WFRD site. The antenna for WES2 is mounted on top of a 10 m steel tower. The

MHR0 antenna is mounted on the roof of the main Millstone Radar building, surrounded by a parking lot. The MHR0 antenna is supported by a crossed pair of 6 inch square sheet metal plates attached to an approximate 2 m tall pole slightly offset from the peak of the Millstone Radar building roof. Clearly, the effect of the antenna mount on PWV estimation is an area in need of more investigation.

7.3 REAL-TIME IONOSPHERIC MEASUREMENT

In the estimation procedure for PWV from GPS data, one of the corrections that must be made is the delay term due to the ionosphere. Because the ionosphere is a dispersive medium, it is usually assumed that the ionospheric term can be directly accounted for by combining the L1 and L2 data. However, even prior to the advent of AS (anti-spoofing), this was never truly the case since a variety of factors, such as multipath and unknown receiver and satellite L1-L2 biases, affect the calculation of the ionospheric correction term from the GPS data. The presence of anti-spoofing further complicates the real-time retrieval of this delay term [25]. Anti-spoofing (AS) and selective availability (SA) are the two techniques that the DoD employs to degrade the accuracy of the GPS system for the non-DoD user. These techniques, and the C/A-code (Coarse/Acquisition) and the P-code (Precision-code), are described in detail in [26]. The majority of GPS receivers are single frequency (L1) C/A code only receivers. This means that AS, which does not affect the C/A code, has no impact on these users, while SA degrades their position accuracy from approximately 25 m to 100 m. This role is reversed in ionospheric determination, where SA has virtually no effect and AS has considerable effect on the determination of the total electron content (TEC) from the GPS data. The next section will briefly discuss how the GPS data are combined to produce the ionospheric delay term. The final section will show how different receivers (in particular the Ashtech Z12 versus the Allen Osborne Turbo Rogue) measure the L1-L2 group delay and integrated phase data in the presence of anti-spoofing.

7.4 GPS MEASUREMENT OF TOTAL ELECTRON CONTENT

The TEC measurement is made by looking at the delay between the L1 and the L2 P-code signals. Both the GPS differential (L1-L2) carrier phase and GPS differential (L1-L2) group delay measurements are used to estimate the TEC. The differential carrier phase data are used to smooth the estimate of the TEC because the phase measurement is extremely precise and is not as corrupted by multipath noise as are the group delay measurements. Unfortunately, the carrier phase data cannot be used to give an absolute determination of the TEC. The carrier phase data are a relative measurement of how the TEC changes as a function of time and position. The differential group delay data must be used to set the absolute level of the TEC.

In ionospheric determination, SA has no effect on the GPS measurement of TEC since the L1 and L2 clocks are dithered in such a way that the effect cancels out when looking at the difference (L1-L2). AS, however, definitely affects P-code receivers. Once AS is turned on, receivers either have to revert to

codeless mode operation [27] or must possess decryption capabilities to decipher the Y code [26]. In codeless mode, the P-code is reconstructed through different algorithms, all of which cost the system a certain amount of signal loss and degradation at low elevations. The AOA Turbo Rogue ICS-4000Z receivers use a cross-correlation signal processing algorithm to reproduce the P-code information. The Ashtech Z12 uses a more sophisticated algorithm. All of the receivers do an acceptable job of recovering the differential carrier phase. The difficulty is in recovering the differential group delay which is needed to obtain the "absolute" value of the TEC. The next two figures, Figures 17a and b, show how well the codeless operation works in these two receivers. The break in the Turbo Rogue carrier phase data merely illustrates the loss of lock frequently present in the carrier phase data.

It is clear that the measurement of the L1-L2 group delay by the Ashtech Z12 system has considerably less noise than that of the AOA Turbo Rogue. The integrated phase measurements of the two systems are nearly indistinguishable, with the exception of the "loss of lock" evidenced in the AOA Turbo Rogue data early in the pass. Subsequent analysis of this data has shown definite improvement in the real-time determination of the TEC using the GRIMS software [28] and the less noisy Ashtech Z12 data versus the AOA Turbo Rogue data. It is critical to recognize that real-time determination of the ionosphere requires the use of the group delay data. The integrated phase data alone cannot provide an absolute measurement of the TEC. Clearly this is a factor that should be considered in the development of near real-time systems for the recovery of PWV.

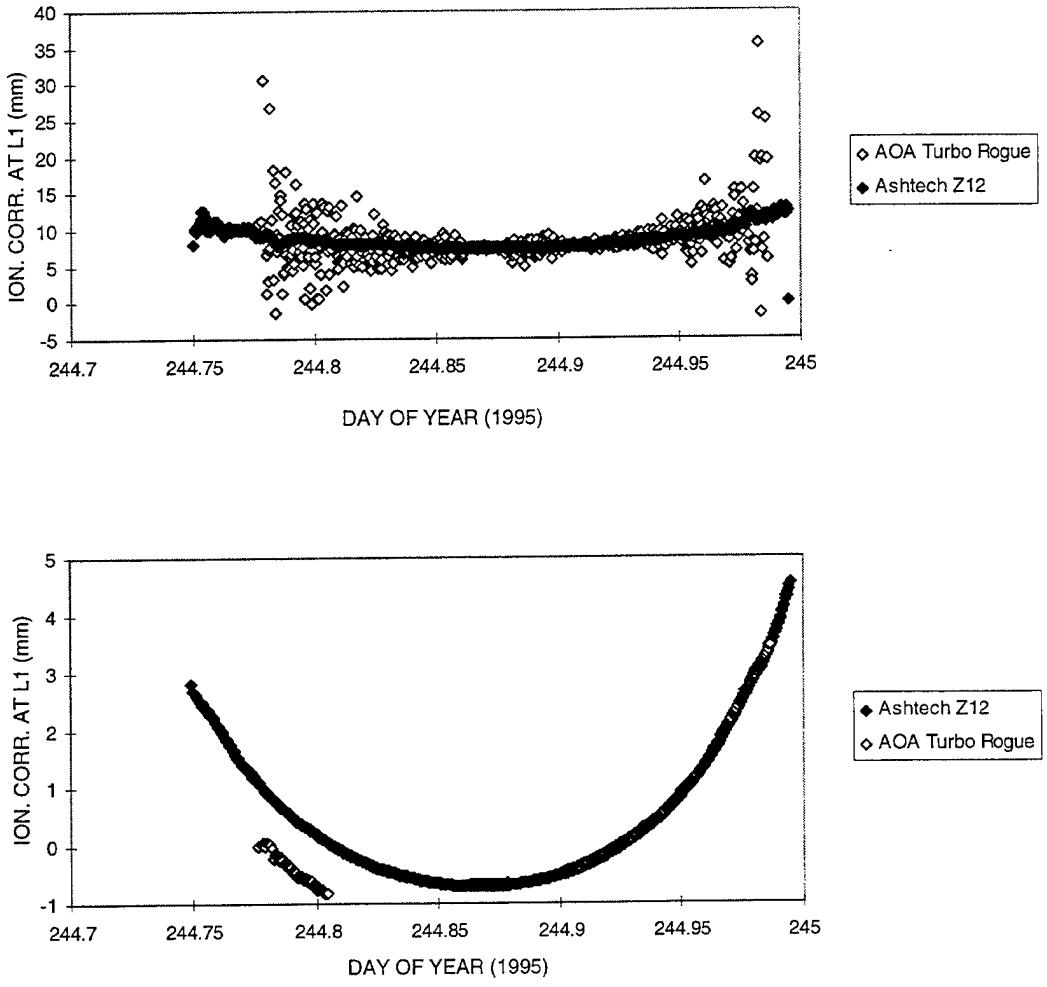

Figures 17a,b. The top plot illustrates the difference in Group Delay Measurements (L1-L2) between the two receivers in codeless mode operation in the presence of Anti-Spoofing. The bottom plot illustrates the difference in their carrier phase measurements.

8. CONCLUSIONS

Based on the analysis of the WWAVE data set, GPS estimates of zenith wet delay agree with measurements by WVR and radiosondes to within 6-12 mm, corresponding to 1-2 mm of PWV. The GPS data used for these accuracy comparisons were all taken with A.O.A. Turbo Rogue GPS receivers using Dorne-Margolin choke ring antennas. Additional GPS data were analyzed using Ashtech Z-12 receivers and either Dorne-Margolin choke ring antennas or their surveying antenna, the 700718B. An elevation cutoff of 5 degrees was used in all of the data processing for instrument comparison. These values of PWV accuracy are consistent with the results of GPS/STORM [6]. The precision of the GPS measurement of ZWD is better than 6 mm (1 mm of PWV) as shown by the agreement of three closely spaced GPS systems. Radiosondes appear to have problems related to their humidity sensors, as indicated in this paper and as discussed in [19]. Radiosondes also cannot provide frequent average measurements of water vapor in a period of rapidly changing weather. Water vapor radiometers have operational problems during rain and may have accuracy restrictions based on their dependence on the radiosonde data to determine their retrieval coefficients. On the other hand, it is important to note that the type of mount, radome, antenna, and receiver used may affect the GPS determination of PWV. The impact of the mounts, antennas, radomes, and receivers on the GPS determination of PWV is an area in need of more investigation.

REFERENCES

1. Y.-H. Kuo, X. Zou, Y.-R. Guo, "Variational Assimilation of Precipitable Water Using a Nonhydrostatic Mesoscale Adjoint Model. Part I: Moisture Retrieval and Sensitivity Experiments," *Monthly Weather Review* ***124***, pp. 122-147 (1996).

2. C. R. Rocken, R. H. Ware, T. Van Hove, F. Solheim, C. Aber, J. Johnson, M. Bevis, S. Businger, "Sensing Atmospheric Water Vapor with the Global Positioning System," *Geophysical Research Letters* ***20***, No. 23, pp. 2631-2634 (December 1993).

3. M. Bevis, S. Businger, S. Chiswell, T. A. Herring, R. A. Anthes, C. Rocken, and R. H. Ware, "GPS Meteorology: Mapping Zenith Wet Delays onto Precipitable Water," *Journal of Applied Meteorology* ***33***, pp. 379-386 (1994).

4. J. L. Davis, T. A. Herring, I. I. Shapiro, A. E. E. Rogers, and G. Elgered, "Geodesy by Radio Interferometry: Effects of Atmospheric Modeling Errors on Estimates of Baseline Length," *Radio Science* ***20***, pp. 1593-1607 (1985).

5. M. Bevis, S. Businger, T. A. Herring, C. Rocken, R. A. Anthes, and R. H. Ware, "GPS Meteorology: Remote Sensing of Atmospheric Water Vapor using the Global Positioning System," *J. Geophys. Res.* ***97***, pp. 15, 787-15, 801 (1992).

6. C. R. Rocken, T. Van Hove, J. Johnson, F. Solheim, R. Ware, M. Bevis, S. Chiswell, and S. Businger, "GPS/STORM—GPS Sensing of Atmospheric Water Vapor for Meteorology," *Journal of Atmospheric and Oceanic Technology* ***12***, pp. 468-478 (1995).

7. A. J. Coster, M. Buonsanto, E. M. Gaposchkin, D. Tetenbaum, and L. E. Thornton, "Ionospheric and Tropospheric Path Delay Obtained from GPS Integrated Phase, Incoherent Scatter and Refractometer Data and from IRI-86," *Adv. Space Res.* ***10***, No. 8, pp. (8)105-(8)108 (1990).

8. A. Dodson, P. Shardlow, "The Global Positioning System as a Passive Integrated Atmospheric Water Vapor Sensing Device," *SPIE* ***2582***, pp. 166-177 (1995).

9. F. H. Webb, and J. F. Zumberge, "An Introduction to GIPSY/OASIS-II," JPL D-11088, California Institute of Technology, Pasadena, California (17 July 1995).

10. A. E. Niell, "Global Mapping Functions for the Atmosphere Delay at Radio Wavelengths," *JGR-Solid Earth* ***101***, B2, pp. 3227-3246 (February 1996).

11. S. M. Lichten, Y. E. Bar-Sever, W. I. Bertiger, M. Heflin, K. Hurst, R. J. Muellerschoen, S. C. Wu, T. P. Yunck, and J. Zumberge, "Gipsy-Oasis II: A High Precision GPS Data Processing System and General Satellite Orbit Analysis Tool," Technology 2005, *Proceedings of NASA Technology Transfer Conference*, Chicago, IL (24-26 Oct. 1995).

12. S. M. Lichten (personal communication, 1996).

13. V. B. Mendes, and R. B. Langley, "Zenith Wet Tropospheric Delay Determination Using Prediction Models: Accuracy Analysis," *Cartografia E Cadastro No. 2 Junho 1995*, pp. 41-47.

14. G. D. Thayer, "An Improved Equation for the Radio Refractive Index of Air," *Radio Science* ***9***, No. 10, pp. 803-807 (1974).

15. G. Elgered, "Tropospheric Radio-Path Delay from Ground-Based Microwave Radiometry," *Atmospheric Remote Sensing by Microwave Radiometry*, Wiley, pp. 215-258 (1993).

16. S. J. Keihm (personal communication, 1995).

17. T. A. Herring, J. L. Davis, and I. Shapiro, "Geodesy by Radio Interferometry: The Application of Kalman Filtering to the Analysis of Very Long Baseline Interferometry Data, *J. Geophys. Res.* ***95***, pp. 12561-12581 (1990).

18. E. R. Westwater, M. Falls, I. A. Popa Fotino, "Ground-Based Microwave Radiometric Observations of Precipitable Water Vapor: A Comparison with Ground Truth from Two Radiosonde Observing Systems," *Journal of Atmospheric and Oceanic Technology* ***6***, pp. 724-730 (1989).

19. C. G. Wade, "An Evaluation of Problems Affecting the Measurement of Low Relative Humidity on the United States Radiosonde," *Journal of Atmospheric and Oceanic Technology* ***11***, pp. 687-700 (1994).

20. A. Jackson, and T. Caudill (personal communication, 1996).

21. F. Solheim, (personal communciation, 1997).

22. J. Ryan (personal communication, 1996).

23. A. E. Niell, R. W. King, S. C. McClusky, T. Herring, "The Effect of Radomes on Dorne-Margolin Choke Ring GPS Antennas," AGU Spring Meeting, Baltimore, Maryland (1996).

24. "Precipitable Water Vapor Comparisons using Various GPS Processing Techniques," Office of Oceanic and Atmospheric Research, Environmental Research Laboratories, Forecast Systems Laboratory, Profiler Program Office, Boulder, Colorado, Document Number 1203-GP-36 (August 28, 1995).

25. P. Gendron, P. Doherty, and J. Klobuchar, "Absolute Real-Time Ionospheric Measurements from GPS Satellites in the Presence of Anti-Spoofing," *Proceedings of the 52nd Annual Meeting of I.O.N. Navigational Technology for the 3rd Millennium,*" Cambridge, MA (1996), pp. 547-556.

26. B. Hofman-Wellenhof, H. Lichtenegger, and J. Collins, GPS Theory and Practice, Springer-Verlag, Wien, Austria (1994).

27. A. J. Van Dierendonick, "Understanding GPS Receiver Terminology: A Tutorial," *GPS World*, pp. 34-44 (January 1995).

28. E. M. Gaposchkin (personal communication, 1997).

REPORT DOCUMENTATION PAGE

Form Approved
OMB No. 0704-0188

1. AGENCY USE ONLY (*Leave blank*)	2. REPORT DATE	3. REPORT TYPE AND DATES COVERED
	17 December 1997	

4. TITLE AND SUBTITLE

The Westford Water Vapor Experiment: Use of GPS to Determine Total Precipitable Water Vapor

5. FUNDING NUMBERS

C — F19628-95-C-0002
PR — 1

6. AUTHOR(S)

Anthea J. Coster
Hsiao-hua K. Burke
Mark G. Czerwinski
Arthur E. Niell

7. PERFORMING ORGANIZATION NAME(S) AND ADDRESS(ES)

Lincoln Laboratory, MIT
244 Wood Street
Lexington, MA 02173-9108

8. PERFORMING ORGANIZATION REPORT NUMBER

TR-1038

9. SPONSORING/MONITORING AGENCY NAME(S) AND ADDRESS(ES)

ESC/ENK
5 Eglin Street
Hanscom AFB, MA 01731-2116

10. SPONSORING/MONITORING AGENCY REPORT NUMBER

ESD-TR-97-060

11. SUPPLEMENTARY NOTES

None

12a. DISTRIBUTION/AVAILABILITY STATEMENT

Approved for public release; distribution is unlimited.

12b. DISTRIBUTION CODE

13. ABSTRACT (*Maximum 200 words*)

The Westford Water Vapor Experiment (WWAVE) was designed to measure the temporal and spatial variability of the total precipitable water vapor (PWV) over an area defined by an approximate 25 km radius centered on the Haystack Observatory in Westford, MA. PWV is defined as the height of liquid water that would result from condensing all the water vapor in a column from the Earth's surface to the top of the atmosphere. The main experiment was conducted from 15 – 30 August 1995, and a variety of different techniques were used to measure the water vapor, including: radiosondes, launched two to three times daily from one location; a water vapor radiometer (WVR); and 11 Global Positioning System (GPS) receivers separated by 0.5 to 35 km. The data were either collected by A.O.A. Turbo Rogue or Ashtech Z12 GPS receivers, and nine sites used choke ring antennas. The WWAVE analysis showed that GPS estimates of zenith wet delay (ZWD) agreed with measurements by the WVR and radiosondes to within 6-12 mm, corresponding to 1-2 mm of PWV. The precision of the GPS measurement of ZWD is better than 6 mm (1 mm of PWV) as shown by the agreement of three closely spaced receivers.

14. SUBJECT TERMS	15. NUMBER OF PAGES 56
	16. PRICE CODE

17. SECURITY CLASSIFICATION OF REPORT	18. SECURITY CLASSIFICATION OF THIS PAGE	19. SECURITY CLASSIFICATION OF ABSTRACT	20. LIMITATION OF ABSTRACT
Unclassified	Same as Report	Same as Report	Same as Report